UNCERTAINTY QUANTIFICATION OF THE SOFAST MIRROR FACET CHARACTERIZATION SYSTEM USING PROBABILISTIC MODELING

Nolan S. Finch[1] and Charles E. Andraka[2]

[1] Sandia National Laboratories, Concentrating Solar Technologies Department, P.O. Box 5800, Albuquerque, NM 87185-1127, USA, +1 (505) 284-5190, nsfinch@sandia.gov

[2] Sandia National Laboratories, Concentrating Solar Technologies Department

Abstract

Sandia Optical Fringe Analysis Slope Tool (SOFAST) is a mirror facet characterization system based on fringe reflection technology that has been applied to dish and heliostat mirror facet development at Sandia National Laboratories and development partner sites. The tool provides a detailed map of mirror facet surface normals as compared to design and fitted surfaces. In addition, the surface fitting process provides insights into systematic facet slope characterization, such as focal lengths, tilts, and twist of the facet.

In this paper, an analysis of SOFAST measurement output sensitivity and uncertainty resultant from input uncertainty is presented for dish facets. System inputs included hardware parameters and setup measurements. Outputs included the fitted facet shape parameters (focal lengths and twist) and the residuals (typically called slope error). In the study, system inputs were treated as random variables and assigned conservative probability distributions. These input variable distributions were then sampled *n*-times according to the Latin Hypercube Sampling method to create *n* SOFAST input decks. Fringe deflection data previously acquired from the measurement of an Advanced Dish Development System (ADDS) structural gore point-focus facet was then combined with the sampled input decks and SOFAST was executed *n*-times to produce *n* results for each SOFAST output. System inputs and outputs were then used in a linear regression model to quantify output sensitivity and uncertainty.

At 95% confidence, results show that SOFAST is capable of characterizing facet focal length within ± 6 mm, facet twist within ± 0.17 mrad/m, global slope error within ± 0.01 mrad RMS, and local slope error within ± 0.17 mrad. As the ADDS point-focus facet is the basis of this study, results reported here are limited to the SOFAST embodiment intended for dish facet characterization.

1. Background

Sandia Optical Fringe Analysis Slope Tool (SOFAST) has been developed for quick, detailed characterization of point focus mirror facets and heliostats [1]. Figure 1 illustrates the SOFAST system setup for an ADDS point-focus facet.

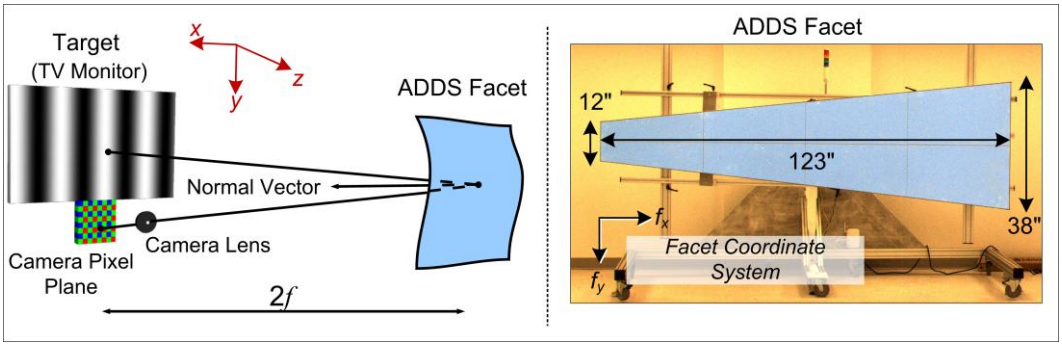

Figure 1. SOFAST system set up illustration (left) and detailed view of ADDS facet used in this study (right). 24 ADDS facets are used to comprise a full ADDS dish system. Each facet utilizes 8 individual mirrors.

In the study presented here, the target is a NEC 70" LCD monitor, the facet is a gore-shaped ADDS facet [2] mounted two focal lengths (2*f*) away, and the camera is a Basler 641fc firewire camera that uses a 2.1 megapixel sensor and a 25mm Fujinon lens. This particular ADDS facet was selected for this study due to its availability and relatively high quality. SOFAST is capable of handling arbitrary facet geometry as defined by the user and is not limited to analyzing ADDS facets.

The fringe reflection technique employed by SOFAST is a dynamic target method that determines surface normals at many points on a facet simultaneously. A camera is pointed at the facet of interest and sees the reflection of the image of an active target – a TV monitor in this case. A series of sinusoidal fringe patterns, or sinusoidally varying brightness patterns (see Figure 1), are displayed on the target and each reflected image is recorded by the camera. Initially, a single cosine wave is displayed and is then shifted three times by 90 degrees each shift. This process provides four brightness levels for each pixel on the camera which are used to determine the phase angle of the target location seen by each camera pixel. The phase angle seen by each camera pixel is used to map each camera pixel to a location on the target. This camera pixel mapping information combined with known camera position and known vectors from each camera pixel to intersection points on the facet surface is used to create a field of facet surface normals. This set of facet surface normals is integrated to a surface shape description. Moreover, the measured surface normals can be fitted to any representative surface shape equation if desired. For the setup used in this study, surface normals were calculated at approximately 480,000 points on the facet.

Correctly calculating the surface normals described above requires accurate measurements of the target (TV monitor) dimensions, camera position relative to the target (translation and rotation), distance from the target to the facet, and the intrinsic camera parameters since a real camera and lens are not accurately represented by a perfect pinhole model (e.g. the camera lens skews incoming light which induces error in SOFAST calculations). The target dimensions and relative positions of the target/camera are quantified with simple tape measurements and a laser distance finder is used to measure the distance from the facet to the target. Camera imperfection is approximated by quantifying the camera's focal length in two axes and estimating the lens distortion with four terms – two radial (barrel) and two tangential. These camera parameters are quantified via a calibration process [3]. The above-mentioned setup and camera calibration parameters are the *inputs* in the sensitivity/uncertainty study presented here. Another source of potential error is the uncertainty of accurately mapping pixels on the camera array to locations on the target as mentioned above. As such, pixel mapping error is also included as an input in this study.

Outputs in the study are the facet characterization results reported by SOFAST which include facet focal lengths in two directions, facet twist in two directions, global slope errors, and local slope errors. Output parameters are calculated by comparing the surface normal data (slope data) obtained by the fringe deflection method to the slope representation of a fitted parabola of revolution [1]. Additional outputs include global slope error and local slope error. Global slope error, more correctly termed the residual, is the root-mean-square (RMS) across all facet points of the difference between the measured data and the model parabola in each axis direction. Local slope error is the slope deviation measured at one point relative to the modeled surface. SOFAST calculates local slope error at all points on the facet and, in this study, results are reported for eight points on the facet (one point from each sub-mirror, see Figure 1) since local deviations are obscured when considering global slope error.

2. Methodology

This is a follow-on study to a linear sensitivity/uncertainty analysis reported in [5]. The previous study estimated uncertainty of SOFAST outputs by calculating linear sensitivities for each output/input combination, assigning conservative uncertainty distributions to each input, creating a linear functionality between each output and all inputs, and using these relationships to bound each output's uncertainty distribution. Since each input was varied by itself while all others were held constant, there were no interactions between input variables – a primary weakness of the method. As such, a more rigorous approach utilizing Latin Hypercube Sampling and regression analysis is presented here.

The approach utilized in this study consisted of acquiring raw slope data from an ADDS facet that had been carefully setup, assigning uncertainty distributions to all input parameters, sampling each input distribution *n*-times to create *n*-input decks, combining the slope data with the *n*-input decks to calculate *n*-results for each SOFAST output variable, and fitting a regression model to the resultant data to assess sensitivity and uncertainty. For clarity's sake, one set of inputs and one set of resultant SOFAST outputs will be referred to as one model realization (one set of acquired slope data is processed *n*-times with *n*-input decks to create *n*-realizations).

The process began by measuring an ADDS facet, whose design focal length (*f*) is 5.33 meters, at three distances: 2*f* , 2*f*+2m, and 2*f*+4m. These acquired slope data provided a baseline for the SOFAST setup. Facet measurement distances farther than 2*f* were considered because these distances result in larger reflected target images and, therefore, will likely have marginally different sensitivities than measurements made in the 2*f* region. Facet measurements were not made closer than 2*f* since doing so would have required a shorter focal length lens for the camera (due to field of view constraints). Switching camera lenses during the analysis would have introduced a host of additional variables and was avoided.

Once the baseline facet measurement data had been collected, input variables were assigned uncertainty distributions. Each input was assigned an uncertainty distribution by analyzing the means by which the input measurement was made. Intrinsic camera calibration parameters (focal lengths and lens distortion coefficients) were calculated by imaging a checkerboard of known dimensions and processing these images with a piece of Sandia-developed software that is based on the CalTech calibration toolbox [3]. Estimates for camera calibration parameters provided by the toolbox also include uncertainty (standard deviation) estimates. These camera uncertainty estimates were used in the SOFAST analysis presented here.

Other inputs included physical measurements of the target dimensions, relative camera/target translations and rotations, and the distance of the facet relative to the target. Target dimensions and target/camera translation measurements were made with a tape measure and were assumed to be accurate within ± 3 mm. The distance from the facet to the target was measured with a laser distance finder whose uncertainty is published to be ± 1.5 mm [4]. Despite this, ± 3mm was used in order to remain conservative.

Target/camera relative rotations were actively driven to zero during setup by squaring the camera to the target. Pitch and yaw were zeroed using a laser square that projected a point onto a wall in front of the camera that represented the intersection of two planes orthogonal to the target. A preview of the camera with a crosshairs superimposed on the field of view was then used to align the camera to the laser projected point. The test setup was squared at a working distance of roughly 15 meters. Estimating the alignment was within two inches in pitch and yaw at this distance gives an uncertainty of ± 3 milliradians. Roll was set by leveling the target then finding a horizontally level fixture (confirmed by measurement) in the field of view of the camera. The camera was then manually rolled until the horizontal crosshair was aligned to the level object in the field of view. Assuming one is able to sight a five-foot fixture and horizontal crosshair to within one inch accuracy at a distance of twelve feet leaves an uncertainty of ± 7 milliradians in roll.

Finally, pixel mapping – the accurate mapping of camera pixels to locations on the target – was assumed to be accurate within ± 2 target pixels based on controlled tests of the SOFAST system. Analysis executed in the previous uncertainty study of SOFAST showed that, due to the large number of points measured, mapping error of individual camera pixels to locations on the target had no impact on any SOFAST output other than local slope errors [5]. Specifically, pixel mapping error sensitivity for local slope errors was found to be 0.002 mrad/pixel. Therefore, in this study, pixel mapping error is only considered for local slope errors and is assigned a uniform uncertainty distribution of ± 2 target pixels centered about zero.

Table 1 below summarizes the uncertainty bands for each input. For reference, Table 2 (also below) shows all SOFAST outputs and their nominal values for an ADDS facet characterization at 2*f*.

Table 1. Summary of SOFAST input parameters and their assigned uncertainy distrbutions

Input Parameter		Nominal	Uncertainty Parameter	Comment
Lens Barrel Distortion Parameter 1	-	-0.1526	σ = 0.0163	Standard Deviation Values Calculated During Camera Calibration
Lens Barrel Distortion Parameter 2	-	1.9414	σ = 0.7686	
Lens Tangential Distortion Parameter 1	-	-0.0002	σ = 0.0002	
Lens Tangential Distortion Parameter 2	-	0.0009	σ = 0.0003	
Camera Focal Length, x	mm	24.02	σ = 0.025	
Camera Focal Length, y	mm	24.00	σ = 0.025	
Target/Camera Rotation, x	radians	0	± 0.003 rad	Uniformly Distributed about Nominal
Target/Camera Rotation, y	radians	0	± 0.003 rad	
Target/Camera Rotation, z	radians	0	± 0.007 rad	
Target/Camera Offset, x	meters	-0.7739	± 3 mm	
Target/Camera Offset, y	meters	0.4304	± 3 mm	
Target/Camera Offset, z	meters	0.0508	± 3 mm	
Target Dimension Horizontal	meters	1.5478	± 3 mm	
Target Dimension Vertical	meters	0.8608	± 3 mm	
Distance from Target to Facet	meters	10.874, 12.877, 14.885	± 3 mm	
Pixel Mapping Error	pixels	0	± 2 pixels	

Table 2. Nominal SOFAST output results for measurement distance 2*f*

Output Parameter	Nominal Value	
Facet Focal Length, X-Direction	5.454	meters
Facet Focal Length, Y-Direction	5.375	meters
Facet Twist, X-Direction	-0.0917	mrad/meter
Facet Twist, Y-Direction	-0.2958	mrad/meter
Global Slope Error	0.8117	mrad
Local Slope Error, Point 1	0.749	mrad
Local Slope Error, Point 2	0.491	mrad
Local Slope Error, Point 3	0.944	mrad
Local Slope Error, Point 4	0.596	mrad
Local Slope Error, Point 5	0.275	mrad
Local Slope Error, Point 6	0.392	mrad
Local Slope Error, Point 7	0.828	mrad
Local Slope Error, Point 8	0.628	mrad

Once distributions had been set for each input variable, each input distribution was sampled via Latin Hypercube Sampling [6] to create many different input variable combinations. Latin Hypercube Sampling was employed over other methods, such as Monte Carlo, because it purposefully pulls equal numbers of samples from equally probable regions of the input uncertainty distribution. Monte Carlo, on the other hand, randomly samples from each input distribution which is prone to clustering and requires many more samples to fully represent the variation of input distribution.

Each input variable combination (i.e. input deck) was then combined with the originally acquired facet slope data and used to run SOFAST and generate output results. SOFAST output variable distributions for each realization were analyzed as the number of sampled input decks was incrementally increased to ensure each sampled output distribution accurately matched its population distribution. Specifically, the number of sampled input decks was increased until it could be shown that each sampled SOFAST output's mean was within 1% of its population mean with > 95% confidence. The details of this calculation are shown in [7]. Ensuring all SOFAST outputs met this criterion required, at minimum, each input distribution to be sampled 4000 times to create 4000 SOFAST input decks. Note that each input deck was combined with the original slope data to produce SOFAST results – only one set of slope data was acquired at each measurement location, not 4000.

After it was verified that enough samples had been taken to ensure the sampled SOFAST output distributions accurately matched their population distributions, a multiple regression model was used to further quantify sensitivity and uncertainty. A linear model was used to relate each SOFAST output (y_i) to all inputs ($x_1, x_2, \ldots, x_n$) as seen in (1):

$$y_i = b_0 + b_1 x_1 + b_2 x_2 + \ldots + b_n x_n \quad (1)$$

The non-standardized regression coefficients (b_i) shown in (1) were calculated by finding the least-squares fit of the SOFAST output data and sampled input data. Calculating standardized regression coefficients (β_i) required a least-squares fit be applied to normalized inputs and outputs as seen in (2) and (3).

$$\hat{y}_i = \beta_0 + \beta_1 \hat{x}_1 + \beta_2 \hat{x}_2 + \ldots + \beta_n \hat{x}_n \quad (2)$$

$$\text{Where: } \hat{y}_i = \frac{y_i - \bar{y}_i}{\sigma_{y_i}} \quad \text{and} \quad \hat{x}_i = \frac{x_i - \bar{x}_i}{\sigma_{x_i}} \quad (3)$$

The standardized regression coefficient (β) is a statistical measure that evaluates the relative contribution (on a normalized basis) of each input parameter to the magnitude of the dependant variable or SOFAST output in this case. The sign of each β also gives the direction of correlation. In short, standardized regression coefficients quantify the sensitivity of each output with respect to each input.

The coefficient of determination (R^2) describes how well a model, like the one shown above, fits measured output data. Values for R^2 range from zero to one with one representing a "perfect" fit (though not necessarily perfect in a causal sense). In order to assess how much each input contributes to the overall output uncertainty, the change in coefficient of determination (ΔR^2) is calculated between the best fit model which includes all of the input terms and a series of models that incrementally drops one input at a time. The importance ranking of the input variables using either ΔR^2 or β is typically the same.

3. Results

The cumulative distribution function (CDF) of facet focal length, x-direction at measurement location 2*f* can be seen in Figure 2. This CDF illustrates the probability of the facet focal length, x-direction falling within a certain range given the uncertainty in all input variables. The plot shows the 95% probable range for facet focal length, x-direction.

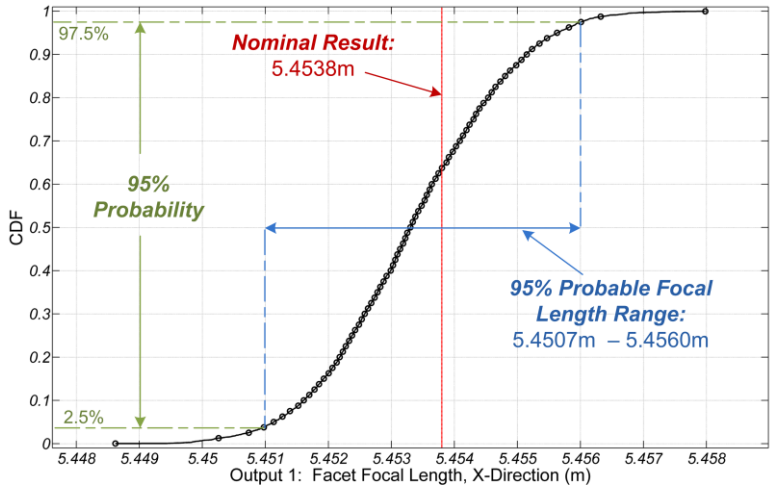

Figure 2. Cumulative distribution function for facet focal length, x-direction at measurement location 2*f*

Due to space constraints, individual CDFs for all outputs at all measurement locations cannot be shown. Figure 3, however, shows the normalized CDFs for facet focal length in both directions, facet twist in both directions, global slope error, and local slope error in both directions for one point on the facet as local slope error data at all eight points were almost identical (all at measurement location 2*f*). Normalized CDFs illustrate the relative uncertainty of SOFAST outputs by placing them all on the same scale. Twist in both directions and local slope error in the y-direction display noticeably more uncertainty than do facet focal lengths and global slope error as evidenced by the linear behavior of their CDFs. Results tabulated in Figure 3 confirm this observation.

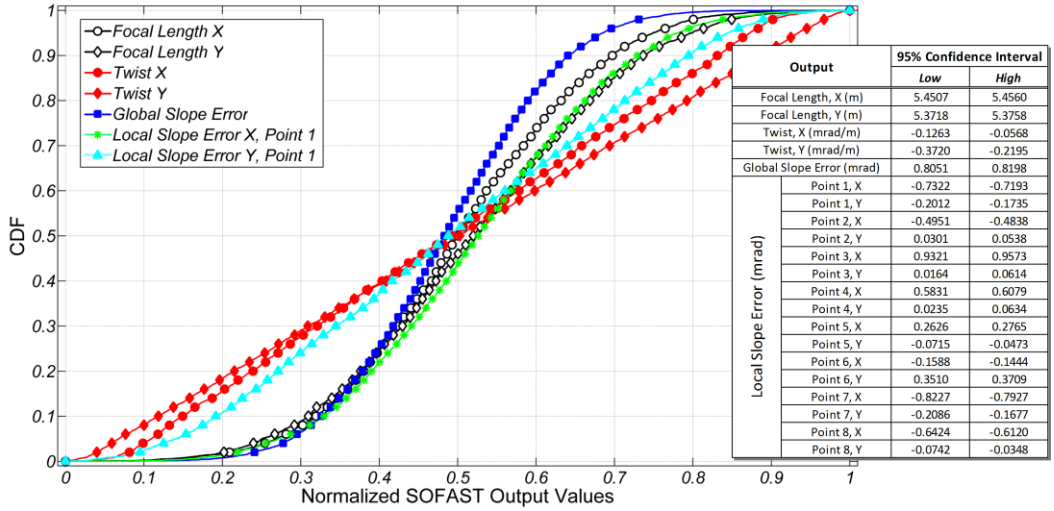

Output		95% Confidence Interval	
		Low	*High*
Focal Length, X (m)		5.4507	5.4560
Focal Length, Y (m)		5.3718	5.3758
Twist, X (mrad/m)		-0.1263	-0.0568
Twist, Y (mrad/m)		-0.3720	-0.2195
Global Slope Error (mrad)		0.8051	0.8198
Local Slope Error (mrad)	Point 1, X	-0.7322	-0.7193
	Point 1, Y	-0.2012	-0.1735
	Point 2, X	-0.4951	-0.4838
	Point 2, Y	0.0301	0.0538
	Point 3, X	0.9321	0.9573
	Point 3, Y	0.0164	0.0614
	Point 4, X	0.5831	0.6079
	Point 4, Y	0.0235	0.0634
	Point 5, X	0.2626	0.2765
	Point 5, Y	-0.0715	-0.0473
	Point 6, X	-0.1588	-0.1444
	Point 6, Y	0.3510	0.3709
	Point 7, X	-0.8227	-0.7927
	Point 7, Y	-0.2086	-0.1677
	Point 8, X	-0.6424	-0.6120
	Point 8, Y	-0.0742	-0.0348

Figure 3. Normalized CDFs and 95% confidence intervals for all outputs at facet measurement location 2*f*

Figures 2 and 3 illustrate SOFAST output uncertainty results for facet data acquired at measurement location 2*f*. As mentioned above, data was also acquired at two other locations: 2*f* , 2*f*+2m, and 2*f*+4m. Uncertainty results for these data are very similar to those shown for the 2*f* measurement locale. Table 3 below shows the worst case 95% confidence intervals for all measurement locations to bound SOFAST output uncertainty for all cases. Maximum local slope error delta (calculated from data taken at all three measurement locations) is reported since nominal values for each subfacet point vary at each measurement location. At 95% confidence and with input uncertainties as stated above, stochastic modeling results show that SOFAST is capable of characterizing facet focal length within ± 6 mm, facet twist within ± 0.17 mrad/m, global slope error within ± 0.01 mrad, and local slope error within ± 0.17 mrad.

Table 3. 95% confidence intervals for all SOFAST outputs for facet measurements taken between 2*f* and 2*f*+4m

Output	95% Confidence Interval		
	Low	*High*	*Delta*
Focal Length, X (m)	5.4507	5.4572	0.0065
Focal Length, Y (m)	5.3634	5.3758	0.0125
Twist, X (mrad/m)	-0.3506	-0.0128	0.3378
Twist, Y (mrad/m)	-0.3720	-0.1077	0.2643
Global Slope Error (mrad)	0.8015	0.8198	0.0184
Max Local Slope Error (mrad)	-	-	0.3380

The prior study mentioned above [5] employed a linear model to assess SOFAST output uncertainty. Each input was individually varied over its uncertainty band, SOFAST was run and outputs logged, and then linear sensitivities between each output/input combination were calculated. These sensitivity values were then combined with input uncertainty distribution information to bound SOFAST output uncertainty. With 95% confidence, results from this prior study indicated facet focal lengths could be

determined within ± 22 mm, facet twist within 0.027 mrad/m, global slope error within ± 0.004 mrad, and local slope error within ± 0.039 mrad. When comparing results from the two methods, all outputs except facet focal lengths showed larger uncertainty when analyzed with the stochastic approach presented here than with the linear approach. This is likely due to the fact that the linear approach did not take input variable interaction into account. As such, the uncertainties estimated by the stochastic approach are likely more reliable.

Results shown to this point have bounded the uncertainty of SOFAST measurement outputs given input uncertainties stated above. In addition to quantifying output uncertainty, it is also important to understand which inputs have the largest impact on output magnitude and output magnitude uncertainty. The standardized regression coefficient (β) quantifies, on a normalized basis, how much each input affects each output's magnitude. The sign of β indicates the direction of correlation. Table 4 shows standardized regression coefficient results for facet measurement location 2*f*. Facet focal length in the x-direction was most affected, all in a normalized sense, by target width, camera focal length in the x-direction, and the distance from the target to facet – all in a positive manner. Facet twist in both directions was almost exclusively affected by the relative rotation of the camera and target in the z-direction (camera roll). A number of inputs affected global slope error – camera focal length x-direction and target width being the biggest contributors. Local slope error was most affected by pixel mapping error, camera roll, camera focal length x-direction, and target width. Relationships shown in Table 4 matched sensitivities calculated in [5] very well which indicates calculations were performed properly. Standardized regression coefficients were also calculated for data taken at the other two facet measurement locations but are not shown here due to space constraints.

Table 4. Standardized regression coefficients (β) for facet measurement location 2*f*

SOFAST Input	SOFAST Output						
	Focal Length, X	Focal Length, Y	Twist, X	Twist, Y	Global Slope Error	Local Slope Error	
						Point 1, X	Point 1, Y
Camera Focal Length, x	***0.520***	0.048	0.088	0.024	***0.692***	***-0.482***	-0.017
Camera Focal Length, y	0.109	***0.276***	-0.086	-0.028	0.034	-0.011	-0.054
Lens Barrel Distortion Parameter 1	0.122	0.057	-0.001	-0.003	***0.202***	-0.027	-0.015
Lens Barrel Distortion Parameter 2	0.080	0.037	-0.004	-0.005	0.156	0.132	-0.006
Lens Tangential Distortion Parameter 1	-0.003	-0.002	-0.003	-0.008	0.001	0.020	-0.004
Lens Tangential Distortion Parameter 2	0.001	0.001	-0.004	-0.002	0.096	-0.065	-0.007
Target/Camera Offset, x	0.006	0.005	0.012	0.004	0.015	-0.013	-0.002
Target/Camera Offset, y	-0.018	0.000	0.001	0.002	0.002	0.000	0.005
Target/Camera Offset, z	0.251	***0.367***	-0.001	0.001	-0.062	0.041	0.005
Target/Camera Rotation, x	0.096	0.164	-0.025	-0.001	-0.014	-0.005	-0.004
Target/Camera Rotation, y	0.046	0.085	0.004	-0.028	0.131	-0.107	-0.052
Target/Camera Rotation, z	0.055	-0.016	***-0.992***	***0.999***	0.197	***-0.394***	***0.953***
Distance from Target to Facet	***0.517***	***0.753***	0.000	0.002	-0.106	0.077	0.009
Target Dimension Horizontal	***0.593***	0.000	0.003	0.005	***0.589***	***-0.495***	-0.002
Target Dimension Vertical	0.011	***0.432***	-0.001	-0.017	0.150	0.000	-0.113
Pixel Mapping Error	0.000	0.000	0.000	0.000	0.000	***0.576***	***0.267***

The effect each input has on the uncertainty of each output is quantified by ΔR^2 – the change in coefficient of correlation between the full regression model and a model lacking the input of interest (β, shown above, quantifies the affect each input has on the magnitude of the output). Table 5 (next page) shows ΔR^2 as a percentage of total ΔR^2 for facet measurement location 2*f*. Uncertainty in facet focal length x-direction is most affected by uncertainty in target width, camera focal length x-direction, and the distance from the target to the facet. Uncertainty in facet focal length y-direction is most affected by uncertainty in facet/target distance and target height. Not surprisingly, facet twist uncertainty was exclusively affected by the relative roll of the camera relative to the target. Uncertainty in global slope error was most affected by uncertainty in camera focal length x-direction and target width. Finally, local slope error uncertainty was driven by uncertainty in relative target/camera roll, pixel mapping error, target width, and camera focal length in the x-direction. ΔR^2 values were calculated at the other two facet measurement locations but are not shown here as the results were very similar to those shown in Table 5.

Table 5. ΔR^2 results for facet measurement location 2*f*

SOFAST Input	SOFAST Output						
	Focal Length, X	Focal Length, Y	Twist, X	Twist, Y	Global Slope Error	Local Slope Error	
						Point 1, X	Point 1, Y
Camera Focal Length, x	***27.0%***	0.2%	0.8%	0.1%	***47.8%***	***23.2%***	0.0%
Camera Focal Length, y	1.2%	7.6%	0.7%	0.1%	0.1%	0.0%	0.3%
Lens Barrel Distortion Parameter 1	1.5%	0.3%	0.0%	0.0%	4.1%	0.1%	0.0%
Lens Barrel Distortion Parameter 2	0.6%	0.1%	0.0%	0.0%	2.4%	1.7%	0.0%
Lens Tangential Distortion Parameter 1	0.0%	0.0%	0.0%	0.0%	0.0%	0.0%	0.0%
Lens Tangential Distortion Parameter 2	0.0%	0.0%	0.0%	0.0%	0.9%	0.4%	0.0%
Target/Camera Offset, x	0.0%	0.0%	0.0%	0.0%	0.0%	0.0%	0.0%
Target/Camera Offset, y	0.0%	0.0%	0.0%	0.0%	0.0%	0.0%	0.0%
Target/Camera Offset, z	6.3%	***13.4%***	0.0%	0.0%	0.4%	0.2%	0.0%
Target/Camera Rotation, x	0.9%	2.7%	0.1%	0.0%	0.0%	0.0%	0.0%
Target/Camera Rotation, y	0.2%	0.7%	0.0%	0.1%	1.7%	1.1%	0.3%
Target/Camera Rotation, z	0.3%	0.0%	***98.3%***	***99.8%***	3.9%	***15.5%***	***90.8%***
Distance from Target to Facet	***26.7%***	***56.6%***	0.0%	0.0%	1.1%	0.6%	0.0%
Target Dimension Horizontal	***35.2%***	0.0%	0.0%	0.0%	***34.7%***	***24.5%***	0.0%
Target Dimension Vertical	0.0%	***18.6%***	0.0%	0.0%	2.3%	0.0%	1.3%
Pixel Mapping Error	0.0%	0.0%	0.0%	0.0%	0.0%	32.9%	***7.1%***

4. Conclusions

SOFAST inputs were treated as random variables with conservative uncertainty distributions, sampled according to Latin Hypercube methodology, combined with three fixed sets of measurement data (one for each facet location), and fed into SOFAST to create output distributions. Output distributions were used to quantify overall SOFAST output uncertainties. A regression model was fit to the data and used to estimate output/input sensitivities (β). This model was also used to determine which input distributions most contributed to each output's uncertainty (ΔR^2). At 95% confidence and with input uncertainties as stated above, results show that SOFAST is capable of characterizing facet focal length within ± 6 mm, facet twist within ± 0.17 mrad/m, global slope error within ± 0.01 mrad RMS, and local slope error within ± 0.17 mrad.

Acknowledgments

Sandia National Laboratories is a multi-program laboratory managed and operated by Sandia Corporation, a wholly owned subsidiary of Lockheed Martin Corporation, for the U.S. Department of Energy's National Nuclear Security Administration under contract DE-AC04-94AL85000. This manuscript has been authored by Sandia Corporation under Contract No. DE-AC04-94AL85000 with the U.S. Department of Energy. The United States Government retains and the publisher, by accepting the article for publication, acknowledges that the United States Government retains a non-exclusive, paid-up, irrevocable, world-wide license to publish or reproduce the published form of this manuscript, or allow others to do so, for United States Government purposes.

References

[1] Andraka, C.E. (2009). "Rapid Reflective Facet Characterization Using Fringe Reflection Techniques", *Energy Sustainability 2009*, San Francisco, CA, USA, July 19-23, 2009.

[2] Diver, R.B., and Andraka, C.E., 2003, "Integration of the Advanced Dish Development System", SAND2003-0780C, *International Solar Energy Conference Proceedings*, Kohala Coast, Hawaii Island, HI, March 15-18.

[3] Bouguet, J-Y., 2008, "Camera Calibration Toolbox for Matlab", http://www.vision.caltech.edu/bouguetj/calib_doc/.

[4] "Leica DISTO D5 Technical Specifications". http://ptd.leica-geosystems.com/en/Leica-DISTO-D5_74709.htm

[5] Finch, N.S., and Andraka, C.E., 2011, "Uncertainty Analysis and Characterization of the SOFAST Mirror Facet Characterization System", *Proceedings of the ASME 2011 5th International Conference on Energy Sustainability*, Paper ES2011-54455, ASME, Washington DC, USA. August 7-10.

[6] Wyss, G.D., Jorgensen, K.H., 1998. "A User's Guide to LHS: Sandia's Latin Hypercube Sampling Software". Sandia National Laboratories, Albuquerque, NM, SAND98-0210.

[7] Ho, C.K. et al., "Methods for Probabilistic Modeling of Concentrating Solar Power Plants". *Sol. Energy (2010)*.